A semi-implicit non-hydrostatic covariant dynamical kernel using spectral representation in the horizontal and a height based vertical coordinate

Juan Simarro and Mariano Hortal
AEMET Agencia Estatal de Meteorología, Spain

2011 EWGLAM/SRNWP Meeting, 10-13 October, Tallinn

Table of contents

1 Introduction

2 Covariant formulation

3 Semi-implicit

4 Tests

5 Conclusions

3D model dynamical core

Main characteritics

- Hybrid vertical coordinate based on height
- Finite differences in the vertical
- Covariant formulation
- Spectral discretization in the horizontal
- Semi-implicit time discretization
- Eulerian or semi-Lagrangian advection

Euler equations for the dry air case

Euler equations

$$\frac{d\mathbf{v}}{dt} + R\,T\,\nabla q + \nabla\phi = \mathbf{F}$$
$$\frac{dr}{dt} + \frac{R}{C_v}\,(\nabla\cdot\mathbf{v}) = \frac{Q}{C_v\,T}$$
$$\frac{dq}{dt} + \frac{C_p}{C_v}\,(\nabla\cdot\mathbf{v}) = \frac{Q}{C_v\,T}$$

- Prognostic variables are $q = \ln p$, $r = \ln T$ and $\mathbf{v} = (u, v, w)$

T is the temperature, p the pressure $\mathbf{v}$ the velocity vector, R is the gas constant for dry air, C_p the specific heat capacity of dry air at constant pressure, C_v the specific heat capacity of dry air at constant volume, $\mathbf{F}(t, x, z)$ is the diabatic momentum forcing, $Q(t, x, z)$ the heat per unit mass and unit time added to the air, $\phi(z) = gz$ the geopotential, $\nabla\phi$ the gradient of geopotential, ∇q the gradient of the logarithm of pressure and $\nabla\cdot\mathbf{v}$ the divergence of the velocity

Prognostic variables

Why $q \equiv \ln p$ and $r \equiv \ln T$?

- Ideal state equation is linear in q, r and $\ln \rho$

$$q = r + \ln \rho + \ln R$$

- Prognostic equations for q and r are linear in prognostic variables in the adiabatic case and have the same forcing terms

$$\frac{dr}{dt} + \frac{R}{C_v} (\nabla \cdot \mathbf{v}) = \frac{Q}{C_v T}$$
$$\frac{dq}{dt} + \frac{C_p}{C_v} (\nabla \cdot \mathbf{v}) = \frac{Q}{C_v T}$$

- For a given time and spatial discretization of $\dot{q}$, $\dot{r}$ and $\nabla \cdot \mathbf{v}$

$$\frac{dq}{dt} - \frac{dr}{dt} = \frac{d}{dt}(q - r) \Rightarrow \frac{d \ln \rho}{dt} + \nabla \cdot \mathbf{v} = 0$$

Model coordinates

- Cartesian (x, y, z) coordinates are transformed into model coordinates (X, Y, Z)
- Vertical domain is $Z \in [0, 1]$ and the horizontal domains are $X \in [-1, 1]$ and $Y \in [-1, 1]$.
- The spatial domain in Cartesian coordinates is bounded by a rigid top at $z = H_T$ and a rigid bottom at $z = H_B(x)$

Domains and grids of physical and model spaces

Representation of the grid

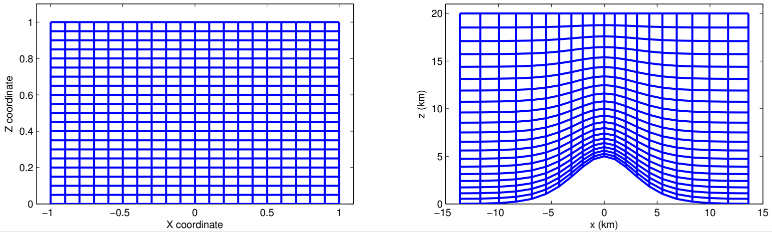

Covariance

- The grid in the model coordinates is regular and it is not in Cartesian coordinates
- The relationship between both coordinates is analytical and constant in time
- The model is covariant in the sense that all the objects are expressed in model coordinates
- The contravariant velocity is chosen as prognostic variable instead covariant velocity because boundary conditions are simply $W(X, Y, 0, t) = 0$ and $W(X, Y, 1, t) = 0$
- Following differential geometry the covariant metric tensor in the new coordinates is all what is needed to express differential operators as divergence, gradient and curl

Metric tensor

- The metric tensor G in the model coordinates is obtained with the help of the Jacobian of the coordinate transformation and the metric tensor in Cartesian coordinates which is the identity

$$G = J^T J$$

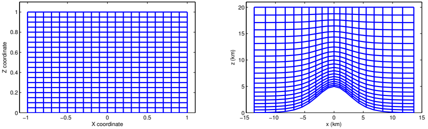

Differential operators

- Differential operators are calculated from the metric tensor and its inverse (G_{ij}, and G^{ij}) and the Christoffel symbols Γ^i_{jk}

$$\Gamma^i_{jk} = \frac{1}{2} G^{im} \left(\frac{G_{mj}}{\partial X^k} + \frac{G_{mk}}{\partial X^j} - \frac{G_{jk}}{\partial X^m} \right)$$

- Divergence

$$\nabla \cdot \mathbf{v} = \frac{1}{|\det G|^{\frac{1}{2}}} \frac{\partial}{\partial X^j} \left(|\det G|^{\frac{1}{2}} U^j \right)$$

- Gradient

$$(\nabla f)^i = G^{ij} \frac{\partial f}{\partial X^j}$$

- Covariant derivative

$$(\nabla_{\mathbf{u}} \mathbf{v})^i = U^j \frac{\partial V^i}{\partial X^j} + \Gamma^i_{jk} U^j V^k$$

Geodesic, parallel transport

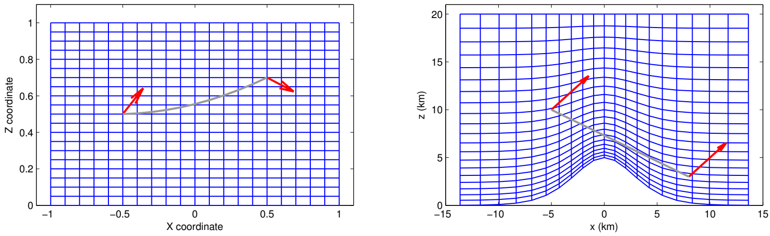

- For the semi-lagrangian advection parallel transport is used for calculating the difference between contravariant vectors at the departure and arrival points
- The trajectory is calculated using a geodesic curve corresponding to the covariant metric tensor
- In this way the semi-lagrangian scheme has a full covariant formulation, in particular the physical velocity components are not used

Vertical discretization

- A 2D VFE version has been coded (paper accepted for publishing at QJRMS, Simarro and Hortal)
- Here a 3D vertical finite differences (VFD) version is presented
- The prognostic variables are all in full levels except the contravariant vertical velocity which is in half levels plus two boundary levels where it is zero
- All the vertical discretization is second order, including those levels near the boundaries

Vertical operators

Basically 4 operators are defined

- $\mathbf{D_Z}$ finds the vertical derivative in full levels and the result is placed in half levels
- $\hat{\mathbf{D}}_\mathbf{Z}$ finds the vertical derivative in half levels considering that the variable is zero at the boundaries and the result is placed in full levels
- $\mathbf{I_Z}$ finds the vertical linear interpolation from full levels to half levels
- $\hat{\mathbf{I}}_\mathbf{Z}$ finds the vertical linear interpolation from half levels to full levels considering that the variable is zero at the boundaries

Semi-implicit time discretization

- The semi-implicit formulation follows closely the formulation used in ALADIN with the mass-based vertical coordinate
- The linear model is around an isothermal hydrostatic balanced atmosphere at rest
- A flat orography is used in the reference state instead of a constant hydrostatic pressure

Linear coordinates

- For the linear system another coordinate transformation is needed which is horizontally uniform
- From this transformation a linear metric tensor G^* is obtained. Consequently the differential operators of the linear model also change.

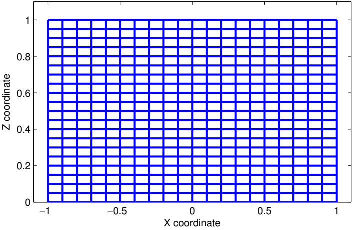

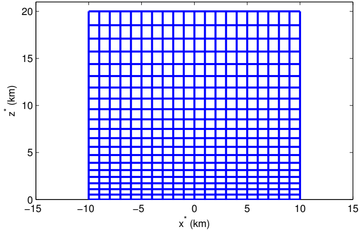

3TL semi-implicit scheme

- A 3TL level scheme is represented by the following equation

$$\frac{\mathbf{X^{n+1}} - \mathbf{X^{n-1}}}{2\Delta t} = \mathbf{M}(\mathbf{X^{n}}) - \mathbf{L}(\mathbf{X^{n}}) + \frac{1-\epsilon}{2}\mathbf{L}(\mathbf{X^{n-1}}) + \frac{1+\epsilon}{2}\mathbf{L}(\mathbf{X^{n+1}})$$

- $\mathbf{M}$ is the non linear model and $\mathbf{L}$ the linear model
- ϵ is a decentering factor which increases stability
- $\mathbf{X} = (\mathbf{U}, \mathbf{V}, \mathbf{W}, \mathbf{r}, \mathbf{q})$ is the state vector
- The linear system is solved for $\mathbf{X^{n+1}}$ in the spectral space

Linear model

$$\frac{\partial \mathbf{U}}{\partial t} + \frac{RT^*}{m_X^2}\mathbf{D_X}\,\mathbf{q} = 0$$

$$\frac{\partial \mathbf{V}}{\partial t} + \frac{RT^*}{m_Y^2}\mathbf{D_Y}\,\mathbf{q} = 0$$

$$\frac{\partial \mathbf{W}}{\partial t} + \frac{RT^*}{m_Z^2}\,\mathbf{D_Z}\,\mathbf{q} - \frac{g}{m_Z}\,\mathbf{I_Z}\,\mathbf{r} = 0$$

$$\frac{\partial \mathbf{r}}{\partial t} + \frac{R}{C_v}\left(\mathbf{D_X}\,\mathbf{U} + \mathbf{D_Y}\,\mathbf{V} + \hat{\mathbf{D}}_\mathbf{Z}\,\mathbf{W}\right) = 0$$

$$\frac{\partial \mathbf{q}}{\partial t} + \frac{C_p}{C_v}\left(\mathbf{D_X}\,\mathbf{U} + \mathbf{D_Y}\,\mathbf{V} + \hat{\mathbf{D}}_\mathbf{Z}\,\mathbf{W}\right) - \frac{m_Z g}{RT^*}\,\hat{\mathbf{I}}_\mathbf{Z}\,\mathbf{W} = 0$$

- m_X^2, m_Y^2 and m_Z^2 are the diagonal elements of the linear metric tensor

Structure equation

- The following structure equation is obtained, which is similar to the structure equation of the ALADIN model

$$\left(\mathbf{I} - \beta^2 c_*^2 \left(\mathbf{D_X^2} + \mathbf{D_Y^2} + \mathbf{L_Z}\right) - \beta^4 c_*^2 N_*^2 \left(\mathbf{D_X^2} + \mathbf{D_Y^2}\right) \mathbf{T_Z}\right) \mathbf{W^{n+1}} = \mathbf{R}_C$$

- where $\mathbf{L_Z}$ and $\mathbf{T_Z}$ are vertical operators which contains vertical derivatives and linear interpolations operators and the constants are

$$c_*^2 = \frac{C_p}{C_v} R T^*$$

$$N_*^2 = \frac{g^2}{C_p T^*}$$

$$H_* = \frac{R T^*}{g}$$

$$\beta = (1 + \epsilon)\,\Delta t$$

Differences with the mass based vertical coordinate

- Contrary to the case of the mass-based vertical coordinate no constraints have to be fulfilled by the vertical operators when deriving the structure equation
- There is not a X term in the divergence due to the use of the contravariant vertical velocity
- The boundary conditions for the contravariant vertical velocity are included in the vertical operators and are automatically fulfilled
- A disadvantage is that the decentering factor must be greater than zero for achieving a similar range of stability (according to the SBH method) than the one obtained with the mass-based coordinate

Test

Following test have been done among others

- Atmosphere at rest with inversion layer (Klemp, 2011)
- Inertia-gravity wave test (Klemp and Skamarock, 1994)
- 3D flow over a hill (Smith, 1980)
- Conservation of potential vorticity

Configuration

- Decentering factor is $\epsilon = 0$
- Reference temperature is $T^* = 350\,K$
- In some test there is an absorber layer in the upper part of the domain to avoid the reflection of gravity waves

Rest atmosphere test

Atmosphere at rest test from Klemp (2011)

- Consist of an atmosphere at rest with a horizontally homogeneous thermodynamic sounding and an orography described in Schär (2002)
- Although the atmosphere is initially in equilibrium at rest an artificial circulation appears during the integration due to numerical pressure gradient errors
- In Klemp (2011) it is used the model described in Klemp et al (2007) with a conservative time-explicit method
- The Gal-Chen (1975) vertical coordinate produced artificial circulations with maximum vertical velocities of $7\,ms^{-1}$
- More sophisticated vertical coordinates results in smaller spurious circulations

Rest atmosphere test: configuration

Configuration

- Constant stability with an inversion layer: $N = 0.01\, s^{-1}$ except $N = 0.02\, s^{-1}$ from $2\, km$ to $3\, km$ height
- Schäer mountain: $H_0 = 1\, km$, $a = 5\, km$ and $b = 4\, km$

$$H_B(x) = H_0 \exp(-\frac{x^2}{a^2}) \cos^2(\frac{\pi x}{b})$$

- Coarse resolution: $\Delta x = \Delta z = 500\, m$
- Gal-Chen vertical coordiante and top placed at $20\, km$
- Diffusion coefficient: $15\, m^2 s^{-1}$
- No vertical sponge zone and cyclic conditions in the horizontal
- Time step $\Delta t = 10\, s$

Rest atmosphere test: maximum vertical velocities

- Atmosphere is initially in equilibrium at rest but artificial circulation appears during the integration due to numerical pressure gradient errors

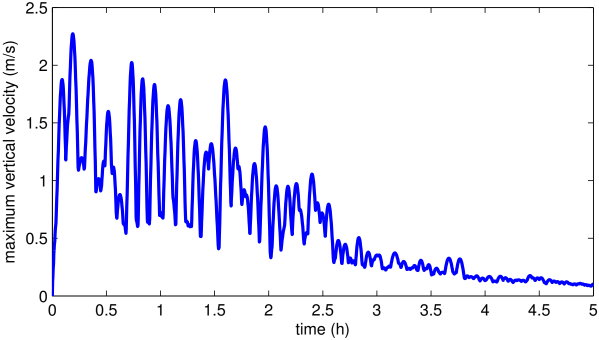

Maximum vertical velocity during the first 5 hours

Rest atmosphere test: potential temperature distortion

- θ isolines are initially horizontal and they are slightly distorted by the spurious circulations

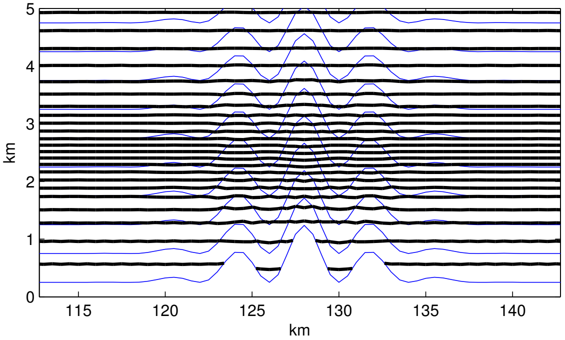

θ after 5 hours of integration and full model levels in blue

Inertia-gravity waves test

Test case found in Skamarock and Klemp (1994)

- There the efficiency and accuracy of the Klemp-Wilhelmson time splitting technique is explored and a propagating inertia-gravity wave is simulated in a Boussinesq atmosphere with constant stability parameter in a periodic channel with solid, free-slip upper and lower boundaries
- The waves are produced by an initial potential temperature perturbation where a small amplitude $\Delta\theta_0 = 0.01\,K$ is chosen for quantitative comparisons with the analytic solutions of the linearized equations

$$\theta(x,z,0) = \Delta\theta_0 \frac{\sin(\pi z)}{1 + \left(\frac{x - x_0}{a}\right)^2}$$

Inertia-gravity waves test: configuration

Configuration

- Constant stability parameter $N = 0.01\, s^{-1}$
- Upper boundary at $H_T = 10\, km$
- Perturbation half width is $a = 5\, km$
- Initial horizontal velocity is $U = 20\, ms^{-1}$
- Horizontal and vertical resolutions are $1000\, m$
- Time step is $\Delta t = 6\, s$.

Inertia-gravity waves test: results

- The numerical solution for θ at $3000\,s$ are similar to the analytical solution, although there is a vertical movement which is not present in the linear Boussinesq solution

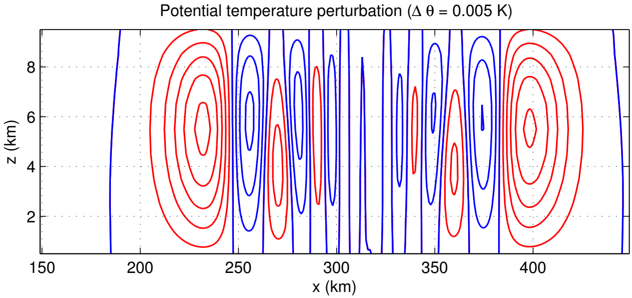

Linear 3D wave test

- Smith (1980) found linear solutions of steady flows which are used here to compare with the nonlinear model solutions

Consider

- steady-state small-amplitude stratified Boussinesq flow
- adiabatic, inviscid and nonrotating
- uniform basic velocity U and Brunt-Vaisala frequency N
- three dimensional topography $H_B(x, y)$

Then the vertical displacement $\eta(x, y, z)$ is given by

$$\left(\frac{\partial^2}{\partial x^2} + \frac{\partial^2}{\partial y^2} + \frac{\partial^2}{\partial z^2}\right)\frac{\partial^2}{\partial x^2}\eta + \frac{N^2}{U^2}\left(\frac{\partial^2}{\partial x^2} + \frac{\partial^2}{\partial y^2}\right)\eta = 0$$

Linear 3D wave test: configuration

Orography: $H_0 = 10\,m$ and $a = 5\,km$

$$H_B(x,y) = \frac{H_0}{\left(1 + \frac{x^2+y^2}{a^2}\right)^{\frac{3}{2}}}$$

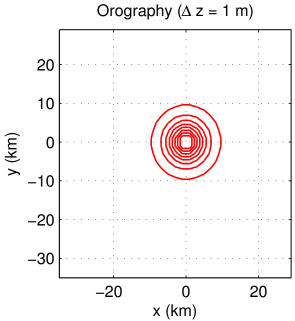

Linear 3D wave test: configuration

Basic state

- $u = 10\, ms^{-1}$ and $N = 0.01 s^{-1}$

Grid and resolution

- Domain: 64×64 grid points in the horizontal and 40 levels
- Resolution: $\Delta x = \Delta y = 2km$ and $\Delta z = 500m$

Linear 3D wave test: linear solution

Linear vertical velocity at level 4 following Smith (1980)

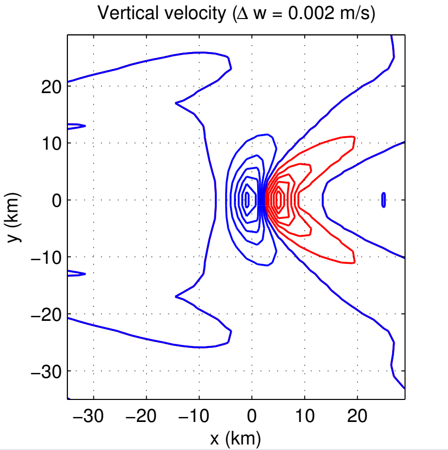

Linear 3D wave test: linear solution

Linear vertical velocity at levels 1, 4, 10 and 20

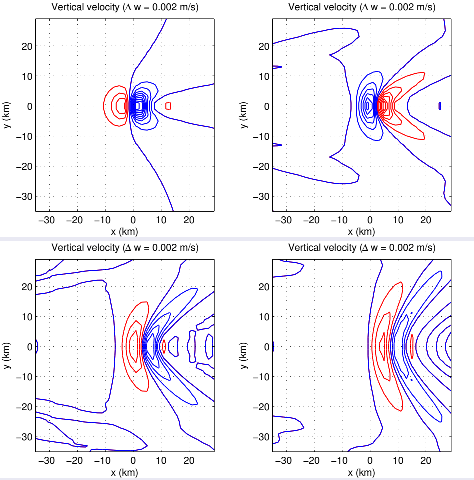

Linear 3D wave test: non linear solution

Configuration

- Same grid used for the linear solution
- Top at $20\,km$
- Time step: $\Delta t = 20\,s$, $\epsilon = 0$
- Reference temperature: $350\,K$
- Cyclic conditions in the horizontal dimensions
- Sponge layer at the highest $4\,km$ of the domain
- Results presented at $T = 30000\,s$

Atention!

- Linear and non linear solutions must be not equal as they obey different equations

Linear 3D wave test: non linear solution

Linear and non linear vertical velocities at levels 1 and 4

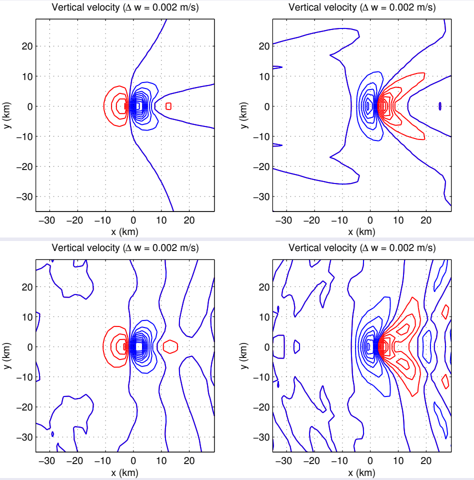

Linear 3D wave test: non linear solution

Linear and non linear vertical velocities at levels 10 and 20

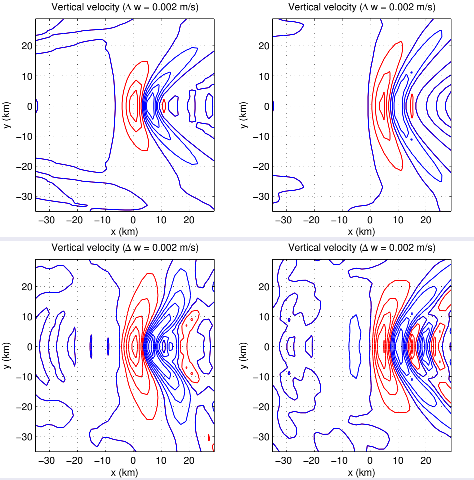

Potential vorticity conservation

Preliminary test to evaluate potential vorticity conservation

- A flow with constant $U = 10\, ms^{-1}$ and $N = 0.01 s^{-1}$ passes around an 3D Agnesi hill $a = 5\, km$ and $H_0 = 500\, m$.
- The flow has zero potential vorticity upstream the hill and should conserve this value in an adiabatic flow
- The potential vorticity is calculated at $T = 3200\, s$
- Two cases: adiabatic case and non adiabatic with heat source. The heat source is proportional to the orography and constant with height, therefore the hill acts like a chimney

Potential vorticity conservation

How to find potential vorticity

- The covariant expression for the potential vorticity is

$$PV = \frac{1}{\rho|G|^{\frac{1}{2}}}\left(\theta_X\left(\hat{V}_Z - \hat{W}_Y\right) + \theta_Y\left(\hat{W}_X - \hat{U}_Z\right) + \theta_Z\left(\hat{U}_Y - \hat{V}_X\right)\right)$$

  where $\hat{U}$, $\hat{V}$ and $\hat{W}$ are the covariant components of the velocity
- Vertical and horizontal derivatives are calculated with respect model coordinates

Potential vorticity conservation

Vertical velocity at 2.5 and $5.0\,km$ height (adiabatic flow up)

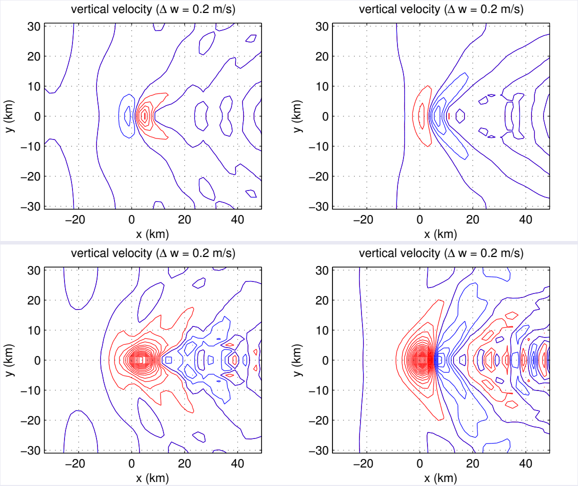

Potential vorticity conservation

Potencial vorticity at 2.5 and $5.0\,km$ height (adiabatic flow up)

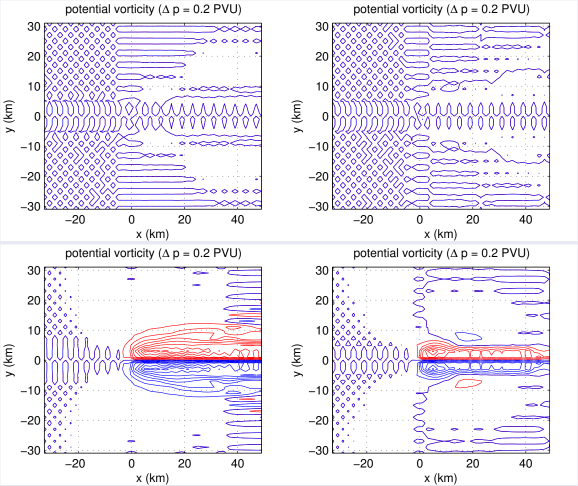

Conclusions

- A 3D VFD model has been coded an tested
- The scheme is robust
- This formulation have some advantages in front of the mass based vertical coordinate
- A preliminary potential vorticity test has been done

Questions (?) and answers (!)

- Work already done in the IFS/HARMONIE code?
  - Preparing inital data in Z coordinate
  - Vertical operators
  - Part of the modifications in the semi-implicit solver
- VFE or VFD?
  - robustness(VFD) $>$ robustness(VFE)
  - VFD to be implemented first
- LAM/Global?
  - First implemented in Global to avoid lateral boundaries

Thank you for your attention!